Cofilin-mediated actin dynamics promotes actin bundle formation during *Drosophila* bristle development

Jing Wu, Heng Wang, Xuan Guo, and Jiong Chen*
State Key Laboratory of Pharmaceutical Biotechnology and MOE Key Laboratory of Model Animals for Disease Study, Model Animal Research Center, Nanjing University, Nanjing 210061, China

ABSTRACT **The actin bundle is an array of linear actin filaments cross-linked by actin-bundling proteins, but its assembly and dynamics are not as well understood as those of the branched actin network. Here we used the *Drosophila* bristle as a model system to study actin bundle formation. We found that cofilin, a major actin disassembly factor of the branched actin network, promotes the formation and positioning of actin bundles in the developing bristles. Loss of function of cofilin or AIP1, a cofactor of cofilin, each resulted in increased F-actin levels and severe defects in actin bundle organization, with the defects from cofilin deficiency being more severe. Further analyses revealed that cofilin likely regulates actin bundle formation and positioning by the following means. First, cofilin promotes a large G-actin pool both locally and globally, likely ensuring rapid actin polymerization for bundle initiation and growth. Second, cofilin limits the size of a nonbundled actin-myosin network to regulate the positioning of actin bundles. Third, cofilin prevents incorrect assembly of branched and myosin-associated actin filament into bundles. Together these results demonstrate that the interaction between the dynamic dendritic actin network and the assembling actin bundles is critical for actin bundle formation and needs to be closely regulated.**

Monitoring Editor
Denise Montell
University of California, Santa Barbara

Received: Feb 16, 2016
Revised: Jun 1, 2016
Accepted: Jun 20, 2016

INTRODUCTION

The actin cytoskeleton is critical for dynamic cellular behaviors such as cell shape change and cell motility. Two types of actin network usually comprise the actin cytoskeleton. The first is a dynamic dendritic network composed of short and loosely held branched actin filaments, and the second is a bundle of a parallel array of long actin filaments tightly clustered by cross-linkers, which is considered to be stable and much less dynamic (Revenu *et al.*, 2004). The dendritic actin network is nucleated and branched by the Arp2/3 complex, and it is maintained as short filaments by the barbed end–capping activity of the capping protein and the filament-severing and pointed end–depolymerizing functions of cofilin/actin-depolymerizing factor (ADF), as occurs in lamellipodia of migrating cells (Revenu *et al.*, 2004). Although the nucleation of bundled actin filaments is less understood, long actin filaments are assembled into actin bundles by the cross-linking activity of various actin-bundling proteins, including fascin and forked in *Drosophila* bristle, villin, fimbrin, and espin in intestinal microvilli, and espin and fimbrin in stereocilia of the inner ear (Bretscher and Weber, 1979, 1980; Tilney *et al.*, 1995; Bartles *et al.*, 1998; Zheng *et al.*, 2000). Of interest, these two vastly different types of actin network often coexist in the same cell type. Can the dynamics of one type of actin network affect the function of the other, and how does this occur? Can the branched actin network be converted into parallel actin bundles or vice versa? Here we used the *Drosophila* bristle cell as a model system to address these questions.

During metamorphosis, the *Drosophila* bristles first sprout from the surface of the thorax 32 h after puparium formation (APF), elongate continuously for 16 h (until 48 h APF) while undergoing dramatic actin bundle assembly, and begin disassembly of actin bundles at 53 h APF (Tilney *et al.*, 1996, 2004; Guild *et al.*, 2002). When the dismantling of actin bundles is complete by 60 h APF, a layer of

This article was published online ahead of print in MBoC in Press (http://www.molbiolcell.org/cgi/doi/10.1091/mbc.E16-02-0084) on July 6, 2016.
*Address correspondence to: Jiong Chen (chenjiong@nju.edu.cn).
Abbreviations used: ADF, actin-depolymerizing factor; AIP1, actin-interacting protein 1; APF, after puparium formation; E-cad, E-cadherin.

cuticle is finished depositing over the surface of the bristle cell, resulting in a grooved pattern in the adult bristles, with the valleys representing regions where membrane-attached actin bundles were previously located and the ridges representing the intervals between any two adjacent actin bundles (Tilney *et al.*, 1996). At the early stage of bristle elongation, two distinct actin filament populations are present at the bristle tip, where robust actin polymerization occurs. A dynamic population of actin filaments, termed "actin snarls" by previous researchers, is mingled with emerging immature actin bundles that begin to be cross-linked by actin-bundling proteins (Tilney *et al.*, 1996, 2003). As bristle elongation proceeds, actin filaments are progressively cross-linked by the bundling proteins forked and fascin in a three-stage process (Tilney *et al.*, 1995, 1996, 2000). As a result, more-mature actin bundles become thicker and are positioned toward the basal region and away from the tip, where new and less-mature bundles are continuously being assembled.

Many mutants in genes required for bundle formation and positioning have been identified by using the alteration of adult bristle morphology as a clue. For example, in *forked* and *singed* (encoding fascin) mutant bristles (Cant *et al.*, 1994; Tilney *et al.*, 1995), actin bundles were greatly reduced in number and size, indicating that the cross-linking activity of these proteins is essential for bundling of actin filaments. An *arp3* (encoding a subunit of Arp2/3 complex) mutation resulted in more parallel ridges on the surface of bristles, reflecting an increased number of actin bundles being positioned at the membrane (Hudson and Cooley, 2002; Frank *et al.*, 2006). Deficiency in *capping protein beta* (*cpb*) caused an increased number of actin bundles that were displaced from the membrane and mislocalized in the internal cytoplasm (Frank *et al.*, 2006). Similar to what occurs in lamellipodia of migratory cells, Arp2/3 complex and capping protein acted antagonistically in the bristles. Of interest, Arp2/3 and capping protein affected the dynamics of actin snarls rather than that of actin bundles, which led to the opposite effects of bundle overpositioning at the membrane and displacement from the membrane in the respective mutants (Frank *et al.*, 2006). However, how actin snarls affect bundle position and whether they affect actin bundle assembly are unknown.

As mentioned, cofilin/ADF acts together with Arp2/3 complex and capping protein to control the dynamics of the dendritic actin network. Cofilin/ADF binds and severs actin filaments, increasing the number of free barbed ends and pointed ends, where polymerization and depolymerization occur, respectively (Maciver *et al.*, 1991; Bamburg, 1999; Wang *et al.*, 2007). Cofilin also enhances the rate of actin monomer (G-actin) depolymerization from the pointed ends of actin filament, resulting in the enlargement of the G-actin pool in vitro (Carlier *et al.*, 1997). Actin-interacting protein 1 (AIP1) is a cofilin-associated cofactor that enhances actin filament disassembly mediated by cofilin (Okada *et al.*, 1999; Rodal *et al.*, 1999). Cofilin and AIP1 are highly conserved across eukaryotes and are essential for many cellular processes requiring strong actin dynamics, such as cell migration, cytokinesis, axon growth, and endocytosis (Bamburg, 1999; Ono, 2003). We previously demonstrated that *Drosophila* cofilin (encoded by the *twinstar* gene) promotes lamellipodial protrusion during cell migration of *Drosophila* border cells, and both cofilin and AIP1 (encoded by *flare*) play essential roles in adherens junction remodeling in the *Drosophila* eye disc epithelium (Chen *et al.*, 2001; Zhang *et al.*, 2011; Chu *et al.*, 2012). Recently we found that murine AIP1 is required both in the germline and in the somatic Sertoli cells for the migration of spermatogonia stem cells in postnatal mouse testis (Xu *et al.*, 2015). These three processes are believed to require disassembly of the dynamic branched actin network. Here we show that cofilin and AIP1 are essential for formation and positioning of actin bundles during bristle development. We find that cofilin promotes the maintenance of a large G-actin pool. Furthermore, cofilin promotes the disassembly of actin snarls, which are found to be associated with myosin II and E-cadherin (E-cad). Loss-of-function analysis of cofilin reveals that actin filaments from such a branched actin-myosin network could be converted or incorporated into actin bundles.

RESULTS

Cofilin and AIP1 are required for *Drosophila* bristle morphogenesis

Previous studies demonstrated that bristle morphological defects reflect the underlying changes in the organization of actin bundles (Tilney and DeRosier, 2005). To determine the requirement of cofilin and AIP1 in bristle development, we first examined the morphology of major bristles, also known as macrochaetes, on the thorax of the *twinstar* (*tsr*; encoding cofilin) and *flare* (*flr*; encoding AIP1) mutant mosaic flies, which were induced by the FRT/Flp system to produce random mutant clones in the adult bodies (Theodosiou and Xu, 1998). Light microscopy and scanning electron microscopy (SEM) images demonstrated that the large bristles in the wild-type (WT) flies (Figure 1, A and L) were long and thin and tapered toward the tip with a slight curve over the thorax. The ridges on the bristle surface were smooth and parallel to each other (Figure 1L). In contrast, in *tsr* and *flr* mutant bristles (Figure 1, B–E and M–O), macrochaetes appeared short and stubby and sometimes bent or split at the tips. SEM images showed that the surface of mutant bristles was rough, and the grooves and ridges were distorted and twisted (Figure 1, M–O). The malformed bristles in the *tsr* mutant appeared more severe than those of *flr* mutants (Figure 1, B–E and M–P). To confirm the mutant bristle phenotype, we also used a bristle-specific *GAL4* (*sca-GAL4*) to drive the expression of *tsr* or *flr* RNA interference (RNAi; *UAS-tsrRNAi* or *UAS-flrRNAi*; Figure 1, F–H). Consistent with the phenotype of mosaic mutant clones, the RNAi flies exhibited very similar bristle morphological defects. All of the 22 macrochaetes on the thorax of *tsr* RNAi flies displayed morphological defects, whereas random mosaic clones induced by heat-shock promoter–driven flippase (*hs-Flp*) displayed defects in only a small portion of the 22 macrochaetes (Figure 1, Q and P). Therefore we chose *sca-GAL4*-driven *UAS-tsrRNAi* flies for subsequent studies. These results demonstrate that both cofilin and AIP1 are essential for bristle morphogenesis.

Next, to further confirm that the phenotype is due to deficiency of cofilin activity, we overexpressed WT or constitutively active form (tsrS3A) of cofilin in *tsr* RNAi–expressing background by using the same *sca*-GAL4driver (Figure 1, I and J). The results showed that a majority of *tsr* RNAi flies could be rescued to appear as WT or close to WT (Figure 1, G, I, J, and Q). In contrast, overexpression of an inactive and phosphomimetic form of cofilin (tsrS3E), in which the serine at position 3 of cofilin is changed to glutamate and which could no longer bind G-actin and F-actin (Bamburg, 1999; Zhang *et al.*, 2011), failed to rescue the bristle phenotype of *tsr RNAi* flies (Figure 1, G, K, and Q). This result shows that the serine phosphorylation site of cofilin and hence cofilin's actin-binding ability are critical for cofilin's function in bristle development.

Cofilin and AIP1 are required for actin bundle formation and localization during bristle morphogenesis

To study the underlying cause of aberrant morphology of bristles, we then examined the actin cytoskeleton of *tsr* and *flr* mutant bristles. In the mature macrochaetes of 48-h-old WT pupae (Figure 2A), actin bundles are aligned parallel to each other near the cell membrane,

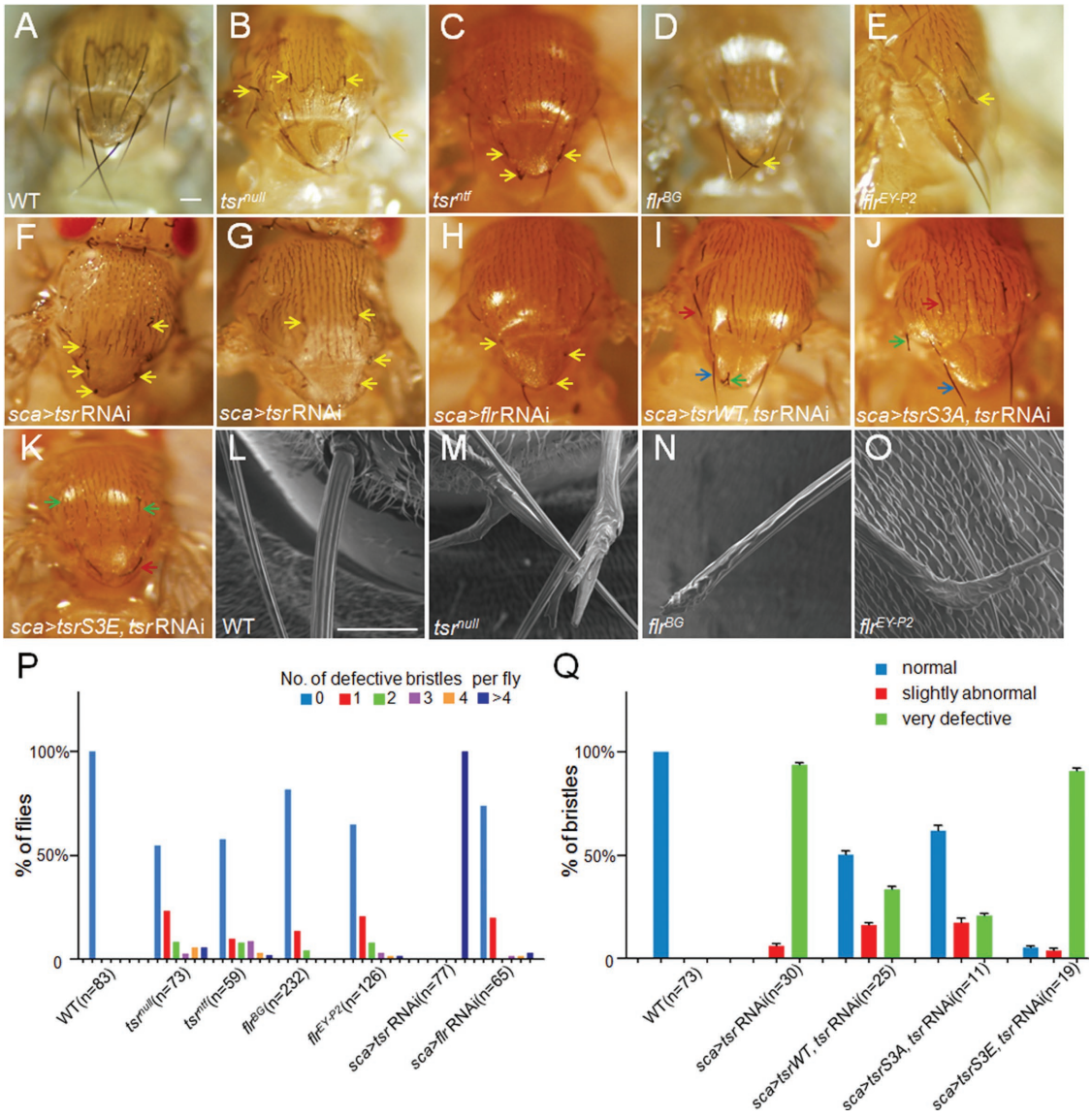

FIGURE 1: Adult bristle phenotypes as caused by *tsr* or *flr* loss of function. (A, L) w^{1118} was chosen as WT control. (B–E) In *tsr* or *flr* mosaic clones, abnormal bristles are indicated by yellow arrows. The mosaic clones of the *tsr* null allele (tsr^{null}) and strong hypomorphic allele (tsr^{ntf}) resulted in more-severe bristle phenotype than those of hypomorphic *flr* alleles (flr^{BG} and $flr^{EY\text{-}P2}$). (F–H) Knockdown of *tsr* or *flr* genes specifically in bristles also resulted in similar bristle defects. (I–K) Abnormal bristle phenotype caused by the knockdown of *tsr* could be rescued by overexpression of WT cofilin (tsrWT) or the constitutively active (CA) form of cofilin (tsrS3A) but not by overexpression of the inactive form of cofilin (tsrS3E). A significant portion of bristles appeared normal (blue arrows) or slightly abnormal (red arrows) in tsrWT- and tsrS3A-expressing flies (I, J), whereas a large majority of bristles appeared severely defective (green arrows) in tsrS3E-expressing flies (K). (L–O) SEM images of adult macrochaetes in WT (L), tsr^{null} mosaic clones (M), and *flr* mosaic clones (N, O). (P) Percentage of adult flies with various defective bristles. Of WT flies, 100% displayed no bristle defects, and none of the 22 macrochaetes appeared defective (blue). In contrast, 0% of *tsr RNAi* flies displayed no bristle defects, and 100% of adult flies had more than four defective bristles (violet). The other genotypes are in between, with a significant percentage of flies displaying no defective bristle (blue), one defective bristle (red), two defective bristles (green column), and so on. Number (*n*) of flies observed is indicated in parentheses. (Q) Effective rescue of bristle defects as caused by *tsr RNAi* by expression of *tsr WT* or *tsr S3A* transgene. For each of the WT flies observed ($n = 73$), 100% of large bristles appeared normal, whereas 0% of bristles in *tsr RNAi* flies ($n = 30$) appeared normal, and 100% of bristles appeared either very defective (green) or slightly abnormal (red). Expression of *tsr WT* ($n = 25$) or *tsr S3A* ($n = 11$) transgene in *tsr RNAi* background on average resulted in at least 50 or 60% of bristles with normal appearance, respectively. Error bars indicate SEM. Bars, 100 μm (A–K), 10 μm (L–O).

with gaps between modules of individual bundle. In tsr^{null} or $flr^{EY\text{-}P2}$ mutant bristles (Figure 2, B and D), the F-actin levels were significantly increased compared with WT (Figure 2H), suggesting more actin bundles. These bundles were arranged in a disorganized manner, however, and they displayed no gaps between modules of bundles. In contrast to the WT bristles, the thickness of actin bundles in the mutant bristles was not uniform and appeared smaller than that of WT bundles, suggesting that the bundle assembly process is

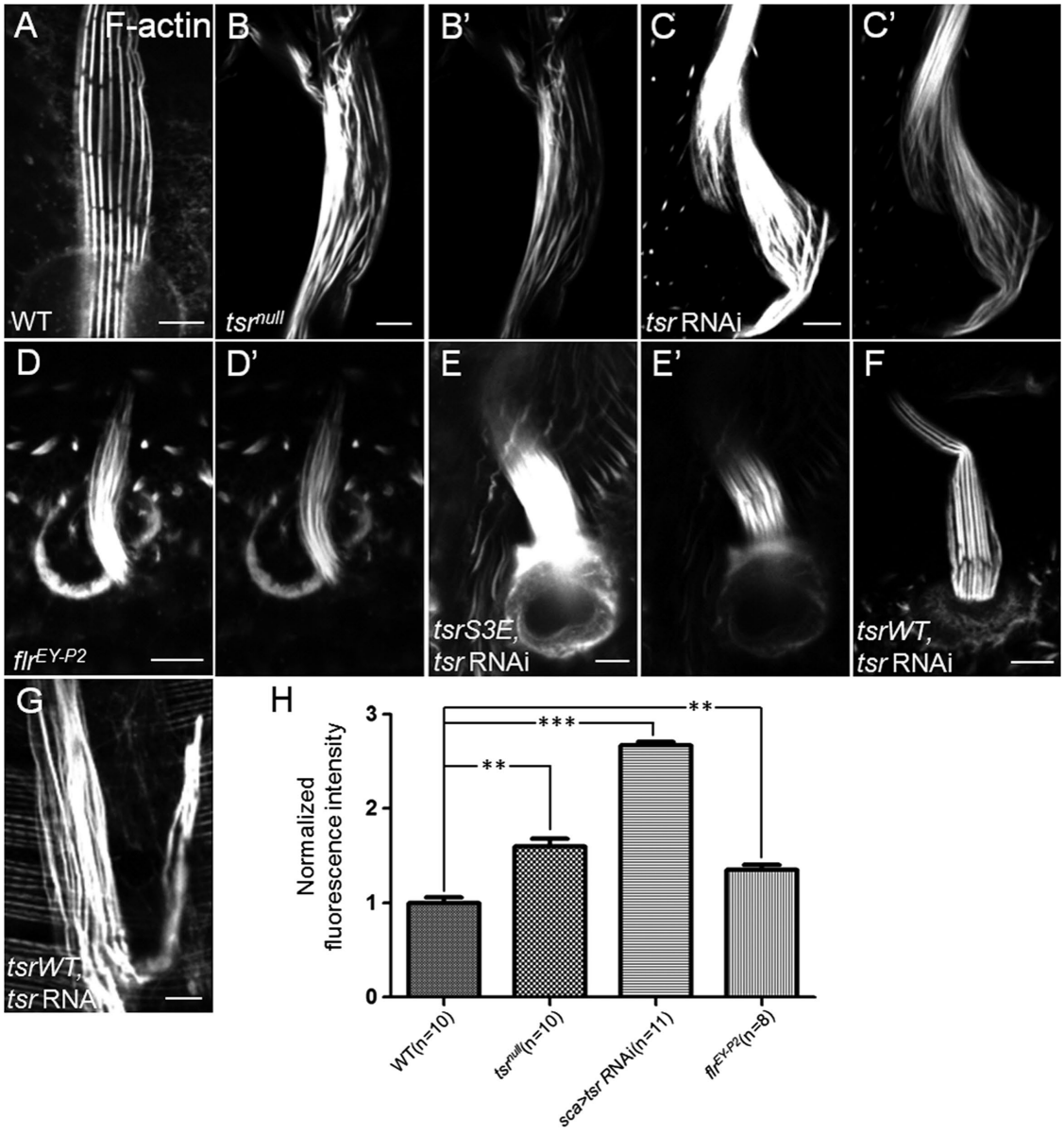

FIGURE 2: Cofilin or AIP1 deficiency resulted in increased F-actin levels and disorganized actin bundles in bristles. (A–D) Confocal micrographs of WT (A), *tsr*-deficient (B, C), and *flr*-deficient (D) bristles at 48 h APF. All bristles were stained for F-actin using rhodamine-phalloidin. These images were taken at the same exposure setting. (B′–D′) Confocal images of the same bristles as B–D, except that they were taken at lower exposure settings to reveal more details of actin bundle organization. (E–G) Confocal micrographs of bristles coexpressing *tsr RNAi* and *tsr S3E* (E, E′) or *tsr RNAi* and *tsr WT* (F, G) at 43h APF. Images in E–G were taken at the same exposure setting. The bristle in E′ was the same as the one in E, but the image was taken at a lower setting to reveal more details. (F) Typical example of a bristle with effective rescue of F-actin level and actin bundle organization by *tsr WT*. (G) Example of a bristle with no full rescue by *tsr WT*. (H) Quantification of F-actin levels of bristles of different genotypes as shown in A–D. The FI of F-actin staining in WT and *tsr*- and *flr*-deficient bristles was measured and normalized against the FI of WT bristles (see *Materials and Methods* for details). The number of bristles measured is indicated in parentheses, and the error bars indicate SEM. $^{**}p < 0.01$; $^{***}p < 0.001$. Bars, 5 μm.

defective in the mutant bristles. Furthermore, actin bundles in bristles of tsr^{null} mosaic flies were more disorganized than those of $flr^{EY\text{-}P2}$ mosaic flies (Figure 2, B and D), consistent with their respective bristle morphological defects. The extent of actin bundle disorganization in *tsr* RNAi bristles was similar to the *tsr* mutant bristles (Figure 2C). Finally, the significant increase of F-actin levels is consistent with cofilin and AIP1 being actin disassembly factors.

Next we found that the WT or S3A form of cofilin significantly rescued the defects of increased F-actin levels and bundle disorganization caused by *tsr RNAi* (Figure 2F and unpublished data), whereas the inactive form of cofilin (tsrS3E) failed to rescue those defects in the tsr *RNAi* background (Figure 2, E and E′). Together the results show that cofilin and AIP1 are required for actin disassembly and bundle formation during bristle development.

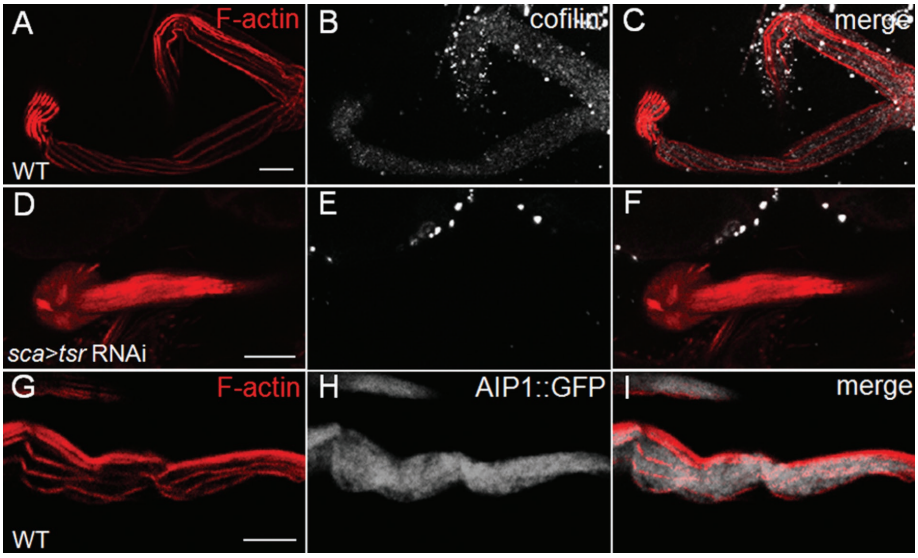

FIGURE 3: Cofilin and AIP1 have uniform distribution patterns in *Drosophila* bristles. (A–F) Mature bristles in WT (A–C) and *tsr RNAi* (D–F) pupae at 48 h APF stained with anti-cofilin antibody (white) and rhodamine-phalloidin (red). Cofilin staining is diffused evenly in the cytoplasm of WT bristles, and lack of staining in *tsr* RNAi bristles indicates good knockdown efficiency. (G–I) Bristle in 43-h-old pupae expressing endogenous AIP1-GFP (white) stained with rhodamine-phalloidin (red). AIP1 is also evenly diffused in WT bristles. Bars, 10 μm.

Cofilin and AIP1 are uniformly distributed in *Drosophila* bristles

To obtain the localization pattern of cofilin in *Drosophila* bristles, we stained the bristles with a previously tested cofilin antibody (Zhang *et al.*, 2011). In WT bristles (Figure 3, A–C), cofilin was evenly distributed throughout the cytoplasm, whereas in *tsr* RNAi bristles (Figure 3, D–F), cofilin staining was absent, indicating that the antibody is specific and RNAi knockdown is efficient. To examine the distribution of AIP1 protein, we used a previously reported *AIP1-GFP* knock-in allele (Figure 3H) that could replace the endogenous AIP1 function and served as a reliable marker for endogenous AIP1 pattern (Chu *et al.*, 2012). The results showed that AIP1 was also uniformly dispersed in the cytoplasm (Figure 3, G–I), similar to the localization of cofilin. These patterns suggest that cofilin and AIP1 are not specifically localized to actin bundles and could act in both bundled and nonbundled actin populations.

Cofilin regulates actin bundle formation and bundle distribution during early stages of bristle development

To determine when actin bundle formation began to be abnormal, we performed phalloidin staining at different stages of bristles development, at 34, 36, 39, 43, and 48 h APF, respectively, for both WT and *tsr RNAi* pupae. Detailed time-course analysis revealed that actin bundle organization and F-actin levels were severely affected in the *tsr* RNAi bristles at the early stages (34 and 36 h APF). In WT, emerging bristles at 34 and 36 h contained ~7–14 actin bundles, which were evenly spaced and distributed in an orderly manner at the cell membrane (Figure 4, A, B, and A1–B2). The other F-actin population, described as "snarls" in previous studies, appeared as moderately stained actin aggregates, which were distributed between actin bundles in the cytoplasm (Figure 4, A and B). In the *tsr RNAi* fly, emerging bristles at 34 and 36 h APF displayed severe disruption in the distribution pattern of actin bundles (Figure 4, F–G′ and F1–G2). First, the number of bundles was greatly increased (Figures 4G′, 5E, and 7E). Second, the bundles were no longer evenly spaced and parallel to each other and no longer distributed near the cell membrane. As a result, disorganized actin bundles filled the cytoplasm of the bristle cell (Figure 4, F1–G2). Third, F-actin levels appeared dramatically increased, as the phalloidin intensity was much higher in *tsr RNAi* than in WT (Figure 4, F and G). Detailed analysis showed that the staining intensity of individual actin bundles appeared to be uneven in comparison to the control but was overall greater than the intensity of the individual control bundle. At later stages (39, 43, and 48 h APF) in WT, more-mature bristles exhibited thicker actin bundles than earlier bristles, consistent with the fact that more actin filaments joined (or become cross-linked to) early bundles to form larger and more-mature actin bundles (Figure 4, C–E). In addition, gaps between modules of actin bundles were a prominent feature of the more-mature bristles (Figure 4, C–E). In the length and width of more mature bristles grew severalfold compared with the early-stage bristles (Figure 4, A–E). In contrast, *tsr RNAi* bristles at the later stages (39, 43, and 48 h APF) displayed a similar bundle thickness to the early bristles (34 and 36 h APF). The bundles failed to grow much larger and thicker compared with the control, and no gaps were detected (Figure 4, F′–J′). Furthermore, the length of *tsr RNAi* bristles was much shorter than those of the WT (Figure 4, A–E and F–J), consistent with its adult bristle morphology. These results suggest that the severe disruption in the actin bundle organization caused by deficiency of cofilin prevented the normal growth or enlargement of the actin bundles and the normal elongation of the bristle, beginning from the early stages.

Reduction of cofilin resulted in reduction of G-actin pool during bristle development

To investigate whether cofilin regulates the G-actin pool in fly bristles, we use DNaseI to label G-actin. In the WT, both early-stage (36 h) and late-stage (48 h) bristles exhibited a largely dispersed distribution of G-actin throughout the cytoplasm (Figure 5, A and G). Moreover, these bristles sometimes displayed strongly stained spots between bundles near the cell membrane (Figure 5, C, C′, I, and I′), indicating enrichment or local high concentration of G-actin there. Of interest, these large spots of G-actin staining exhibited good colocalization with actin snarls in the early bristles (Figure 5, A–C; compare with Figure 6, F–H). In the *tsr RNAi* fly, the large spots of G-actin staining almost totally disappeared, and the overall G-actin levels were significantly reduced in both early-stage (36 h) and late-stage (48 h) bristles, as indicated by DNaseI staining and fluorescence intensity quantification (Figure 5, D, J, and M). Of interest, cross-sectional views showed that G-actin and actin bundles had a largely complementary distribution pattern, with G-actin mainly localized near the cell membrane and disorganized bundles mainly localized at the center of the bristle cell (Figure 5, F′ and L′). These results show that cofilin promotes a local high concentration of G-actin in the early stage of actin bundle formation and also promotes a strong global level of G-actin throughout the stages of bundle formation.

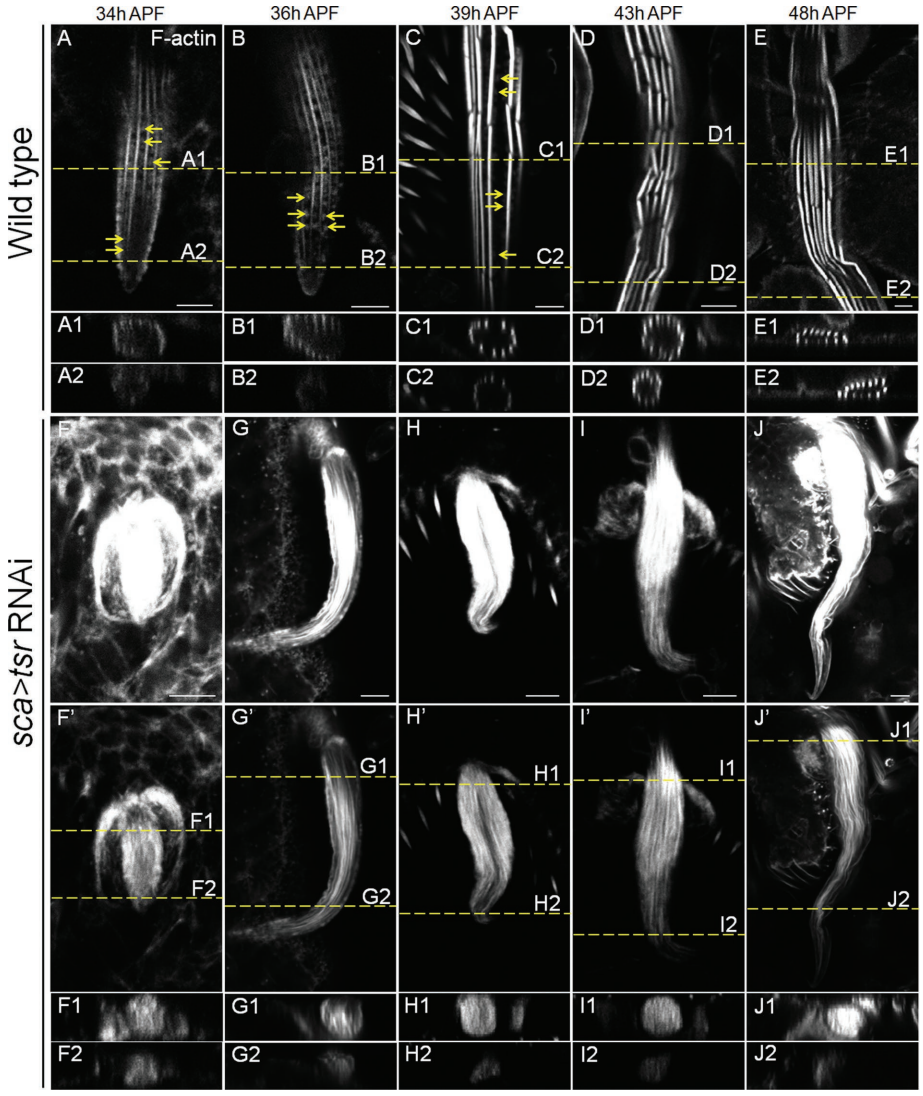

FIGURE 4: Cofilin loss of function resulted in excessive accumulation of actin bundles at the early stages of *Drosophila* bristle development. (A–J) Time-course analysis of actin bundle formation from 34 to 48 h APF in WT (A–E) and *tsr RNAi* (F–J, F′–J′) bristles. A *z*-series of confocal sections was obtained for each bristle. A confocal section at the level showing most actin bundles in one view is shown as a representative image for each time point, and two cross-sectional views (generated from the *z*-series) at two different positions (yellow dashed lines) along the bristle are shown underneath. Images in A–E and F–J were taken at the same exposure setting to compare their F-actin levels, and images and *z*-series (and thus cross-sectional views) in F′–J′ were taken at lower exposure settings than in F–J to reveal more details of bundle organization. The *sca-GAL4* flies were used as WT controls (A–E) to compare to *sca-GAL4, UAS-tsrRNAi* flies (F–J). F-actin of bristles was stained with rhodamine-phalloidin (white). Yellow arrows point to actin snarls between the bundles in A–C. Bars, 5 μm.

We then examined the effect of cofilin loss of function on this distinct actin population. Rhodamine-phalloidin staining of WT fly bristles revealed that the "snarl" structures of F-actin were strongly present within the emerging bristles at 32–36 h APF (Figures 4B and 6, A′ and F–H), consistent with previous reports (Tilney *et al.*, 2003; Frank *et al.*, 2006). The actin snarls were strongly localized at the tip of emerging bristles and were present at the regions between adjacent actin bundles near the membrane. However, actin snarls were present between bundles in a significant amount within the more-mature bristles (39–48 h APF; Figure 6, B–D′), contrary to findings from the previous reports. Whereas lower exposure settings in the confocal microscopy sometimes resulted in the appearance of no F-actin staining between the bundles, increased exposure coupled with more sensitive confocal detectors (see *Materials and Methods*) revealed the clear presence of a snarled or mesh-like network of F-actin between the bundles (Figure 6, C and D′). Furthermore, labeling the F-actin by Lifeact–green fluorescent protein (GFP), which is specifically expressed in the bristles by *Sca-Gal4*, also confirmed the existence of a significant level of actin snarls in later stages (Figure 6, E and E′). Therefore we believe that the lack of detection of actin snarls in previous studies is probably due to the use of lower exposure settings (compare Figure 6, C to C′), less sensitive detectors, or the very high level of F-actin within bundles concealing the relatively low level of F-actin in the actin snarls. In the *tsr RNAi* bristles from 34 to 48 h APF, the actin snarls could not be easily identified because the disrupted positioning of excessive actin bundles and the strongly increased F-actin levels in the disorganized bundles resulted in little space between bundles, making imaging between strongly stained bundles very difficult. In an effort to identify markers that could be associated with actin snarls, we discovered Sqh (myosin II light chain) to be strongly colocalized with actin snarls during both early and late stages of actin bundle assembly (Figures 6, F–H, and 7). In WT bristles, both Sqh-GFP and Sqh-mCherry displayed a complementary localization pattern to that of the actin bundles and were colocalized with actin snarls between any two adjacent bundles near the membrane (Figure 7 and Supplemental Figure S1). To determine whether this localization pattern of myosin II is specific, we also examined the distribution pattern of a number of cytoskeletal proteins, including tubulin and the aforementioned cofilin and AIP1 (Figures 3 and 8, A–C). We found that tubulin's localization (like that of cofilin and AIP1) was uniform and diffused throughout the cytoplasm of the bristle cell (Figure 8, A–C), which was very different from the evenly spaced distribution pattern of myosin II. Of interest, in *tsr RNAi* bristles, the

Reduction of cofilin resulted in excessive polymerization of myosin-associated actin filaments, which were incorporated into actin bundles

Previous work showed that besides actin bundles, a second actin population called actin snarls was present in the emerging bristles at early stage of bristle development (Tilney *et al.*, 1996, 2003) and disappeared during later stages of bundle assembly. Actin snarls were reported to be dynamic actin structures (Tilney *et al.*, 1996, 2003), their assembly and disassembly were mediated by Arp2/3 complex and capping protein, respectively, and their misregulation affected the positioning of actin bundles during bristle development (Frank *et al.*, 2006).

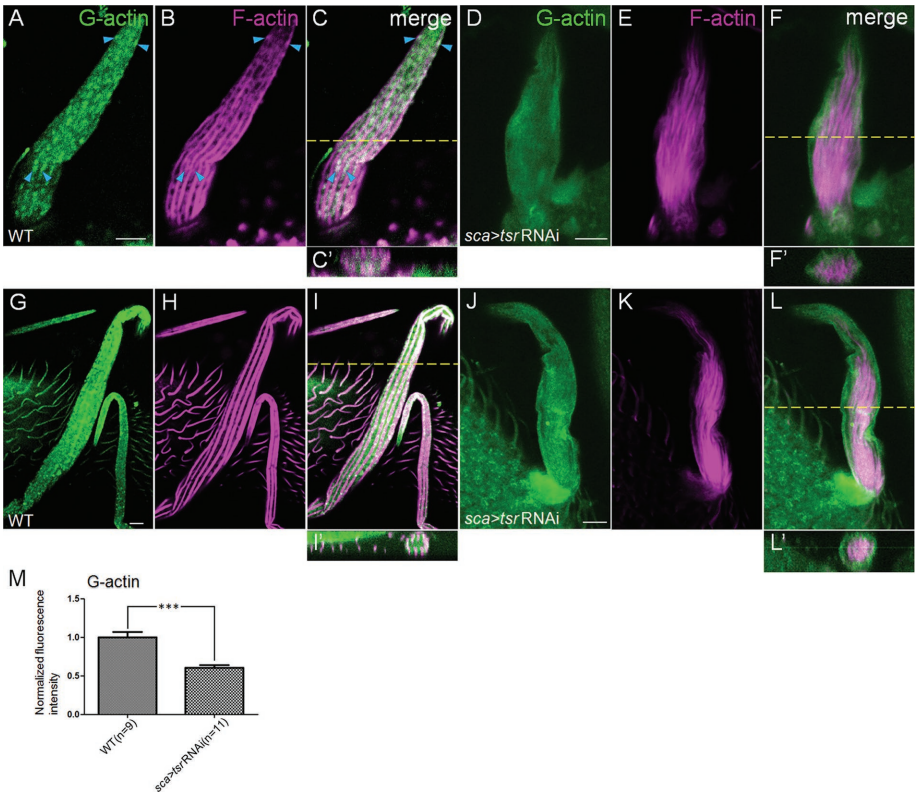

FIGURE 5: Cofilin promotes the G-actin pool during bristle development. (A–L) Confocal micrographs of early-stage WT (A-C) and *tsr RNAi* (D–F) bristles at 36 h APF and late-stage WT (G–I) and *tsr* RNAi (J–L) bristles at 48 h APF, which were stained for DNaseI (green) and rhodamine-phalloidin (magenta). A *z*-series of confocal sections was obtained for each bristle. A confocal section at the level showing most actin bundles near the membrane is shown as a representative image for each bristle, and one cross-sectional view (generated from the *z*-series) at a position (yellow dashed line) along each bristle is shown underneath (C′, F′, I′, L′). Images in A–C and D–F or images in G–I and J–L were taken at the same exposure settings to compare their G-actin levels. Blue arrowheads in A–C point to representative colocalization of G-actin with nonbundled F-actin snarls. (M) Quantification of G-actin levels of bristles from WT and *tsr RNAi* pupae as in G–L. The FI of G-actin staining in *tsr RNAi* bristles was measured and normalized against FI of WT bristles (see *Materials and Methods* for details). Number of bristles measured is indicated in parentheses, and error bars indicate SEM. ***$p < 0.001$. Bars, 5 μm.

localization of myosin II was dramatically altered. Instead of localizing complementarily to the bundles near the membrane, myosin II was now mostly colocalized with the excessive actin bundles in the internal regions of the cytoplasm (Figure 7, D–F, J–L, P–R, and V–X). Of interest, this colocalization of myosin II with disorganized actin bundles began at an early stage of actin bundle formation (34 h) and persisted throughout the later stages of bundle assembly (39–48 h APF). Together these results suggest that the actin-myosin network or actin snarls in WT bristles can be entirely converted or incorporated into actin bundles when cofilin is not present.

E-cadherin localizes between actin bundles in the wild type and localizes onto the bundles in cofilin-deficient bristles

In an attempt to identify additional factors associated specifically with the actin-myosin network, we found E-cad, a transmembrane adhesion protein, colocalized with actin snarls. Similar to myosin II, E-cad had a complementary distribution pattern to that of actin bundles at the membrane (Figure 8, D–I). Both *ubi* promoter–driven E-cad–GFP and the endogenous E-cad–GFP (knock-in allele) localized between the adjacent actin bundles at the membrane of the WT bristles. In *tsr RNAi* bristles, E-cad–GFP (knock-in) lost the membrane-associated localization and was mostly colocalized with the disorganized actin bundles throughout the cytoplasm (Figure 8, J–L) in a similar manner to that of myosin II. However, knockdown of *E-cad* using two different *RNAi* lines (Vienna *Drosophila* Resource Center line 27081 and Tsinghua University RNAi Stock Center line THU2775) resulted in no significant defects in the adult bristle morphology, raising the possibility that the knockdown may not be effective in the bristles.

DISCUSSION

Our data demonstrate that cofilin likely promotes actin bundle assembly and positioning during bristle development in the following ways. First, cofilin promotes a high concentration or a large pool of G-actin both locally (near actin snarls) and globally (throughout the cytoplasm) in the elongating bristles. By ensuring an abundant supply of G-actin, rapid actin polymerization could take place where initial bundles are formed, which is close to the tip of emerging bristles. Of interest, the colocalization of large spots of G-actin with actin snarls near the membrane of early-stage bristles suggests that the local high level of G-actin results from the depolymerization of actin snarls by cofilin (Figure 5, A–C). Indeed, a deficiency of cofilin resulted in the loss of the local enrichment of G-actin near the membrane at the tip (Figure 5, D–F). In addition, a robust level of G-actin globally could also help the assembly of the more-mature bundles by promoting constant polymerization of actin filaments that need to be continuously incorporated into growing bundles throughout the stages of bundle assembly. Second, cofilin acts to limit the size of actin snarls, or the actin-myosin network, by promoting the turnover of actin snarls. Previous studies showed that the Arp2/3 complex and capping protein also regulated the dynamics of actin snarls (Frank *et al.*, 2006), suggesting that this actin population must have been composed of branched actin filaments. Indeed, we observed that this actin population, which was localized between any two adjacent actin bundles, had a mesh-like appearance (Figure 6D), consistent with its being a branched actin network. Without cofilin, this actin network became excessively polymerized, interfering with the localization of the evenly spaced actin bundles near the membrane. Therefore cofilin's function could be to limit this actin-myosin network to a proper size, ensuring the correct positioning of actin bundles.

Of interest, the cofilin loss of function uncovered an unexpected phenomenon: the branched and myosin-associated actin network could be entirely converted or incorporated into actin bundles, which are usually considered as linear arrays of actin filaments bundled together by cross-linkers. This began in the early phase of actin bundle formation and lasted throughout later stages of bundle assembly, since from 34 to 48 h APF, nonmuscle myosin II was mostly colocalized with the disorganized actin bundles in the internal regions of cytoplasm. In WT bristles, myosin II did not display any

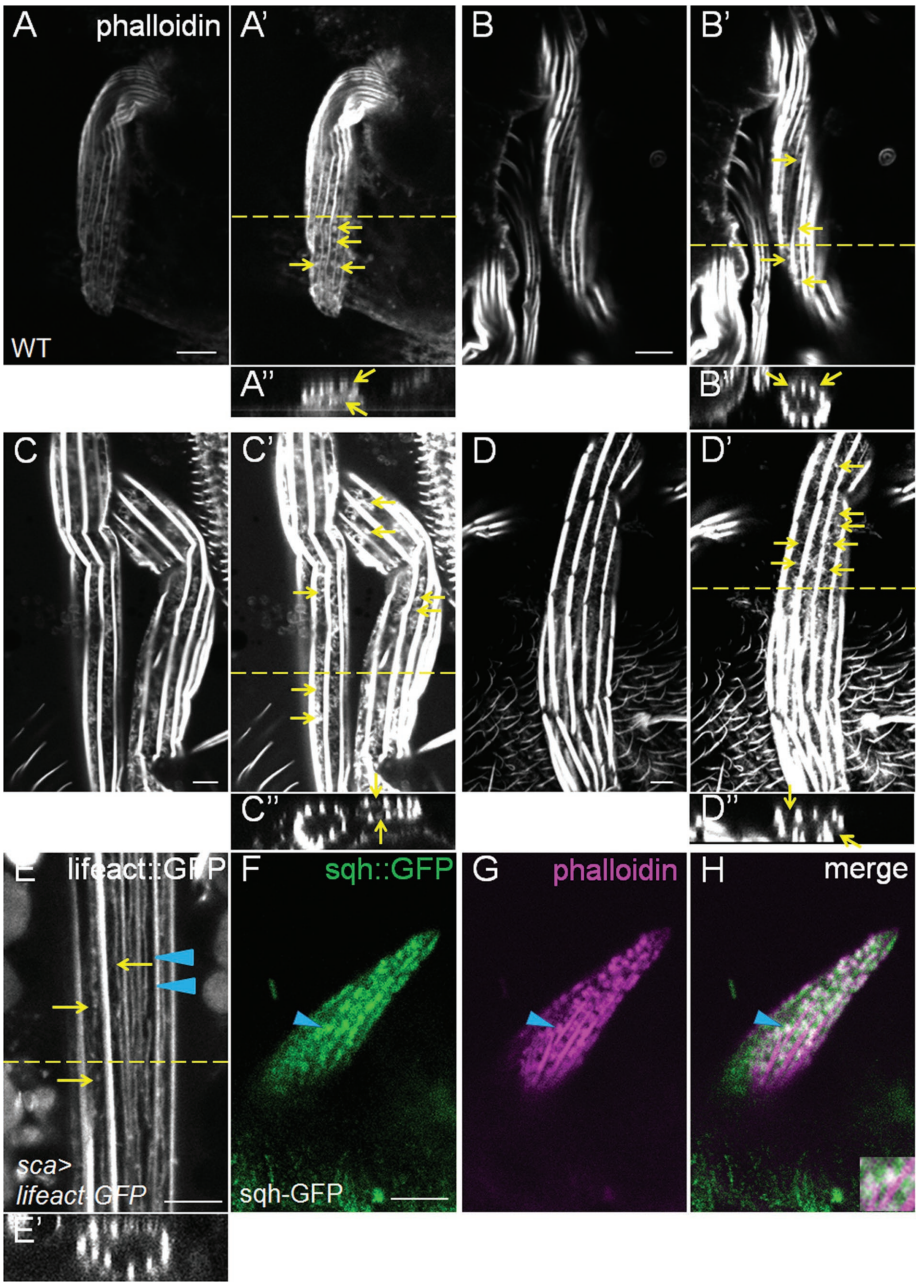

FIGURE 6: Nonbundled F-actin snarls persisted throughout different stages of bundle assembly. (A–D′) Phalloidin staining revealed the presence of actin snarls (yellow arrows) between adjacent actin bundles at 34 (A, A′), 39 (B, B′), 43 (C, C′), and 48 h (D, D′) APF. Confocal images captured at increased exposure settings (A′–D′) clearly show the significant staining of actin snarls, whereas images taken at lower settings sometime failed to clearly show it (e.g., compare C′ to C). (A″–D″) Cross-sectional views. (E) Lifeact-GFP clearly labels two distinct populations of F-actin—actin bundles (blue arrowheads) and actin snarls (yellow arrows)—in a 43–h APF bristle. (E′) Cross-sectional view. (F–H) Newly emerging bristle of WT pupa expressing *sqh-GFP* (green) at 32 h APF stained with phalloidin (magenta). At the tip of this very young bristle, Sqh (myosin II) colocalizes strongly with actin snarls but not with thin actin bundles that were newly bundled and immature. Bars, 5 μm.

colocalization with actin bundles but instead was colocalized with actin snarls. These data suggested that excessively polymerized actin filaments within the actin-myosin network could be incorporated and cross-linked (by cross-linkers such as fascin and forked) into actin bundles. Therefore the third role of cofilin is to keep these two actin populations separate by limiting the actin-myosin network to a small size, preventing incorrect assembly of long-branched actin filament into bundles.

What, then, are the WT roles of the actin-myosin network during bundle assembly? First, as mentioned earlier, this population of F-actin is critical to determining the positioning of developing actin bundles in the bristles. Frank *et al.* (2006) proposed that actin snarls regulate the number and spacing of actin bundles by competing with initial bundles for binding sites at the membrane. How the competition takes place is not known. Of interest, we found that E-cad, which is a transmembrane adhesion protein, is also localized (together with the actin-myosin network) between any two adjacent actin bundles along the WT bristle membrane. In cofilin-deficient bristles, however, E-cad and myosin II are mostly localized in the disorganized actin bundles. These results suggest that actin-myosin network that is coupled to membrane-bound E-cad could be used in a positioning mechanism to limit developing bundles to an evenly spaced localization pattern at the membrane. Furthermore, the presence of myosin II raises the possibility that contractile forces between the membrane and bundles as provided by the actin-myosin mesh somehow could be involved in such a positioning mechanism.

Moreover, the actin snarls could serve as local reservoirs for high levels of G-actin and short actin filaments, which are then conveniently located next to the initial bundles in the emerging bristles and adjacent to the more-mature bundles in later-stage bristles. A constant supply of G-actin and severed short filaments resulting from cofilin's depolymerizing and severing activities could locally drive the high level of actin polymerization during different stages of bundle assembly. Despite extensive researches in bristle development, how bundled actin filaments are nucleated and polymerized during actin bundle formation remains largely unknown. It is clear from previous work that Arp2/3 do not serve as actin-nucleating agents for linear arrays of bundled actin filaments (Frank *et al.*, 2006). Our aforementioned finding that myosin II–associated actin snarls could be almost entirely converted into disorganized bundles during the initial bundle assembly stage of cofilin-deficient bristles suggests that actin snarls somehow contribute to actin filaments of the initial bundles in the emerging WT bristles. Indeed, the actin-myosin network was strongly present in the tip of emerging bristles at 32 and 34 h APF (Figure 6, F–H), where polymerization of actin filaments to be bundled is supposed to occur. Of importance, this actin-myosin population continued its significant presence throughout the later bundle assembly stages, from 36 to 48 h APF. It is noteworthy that

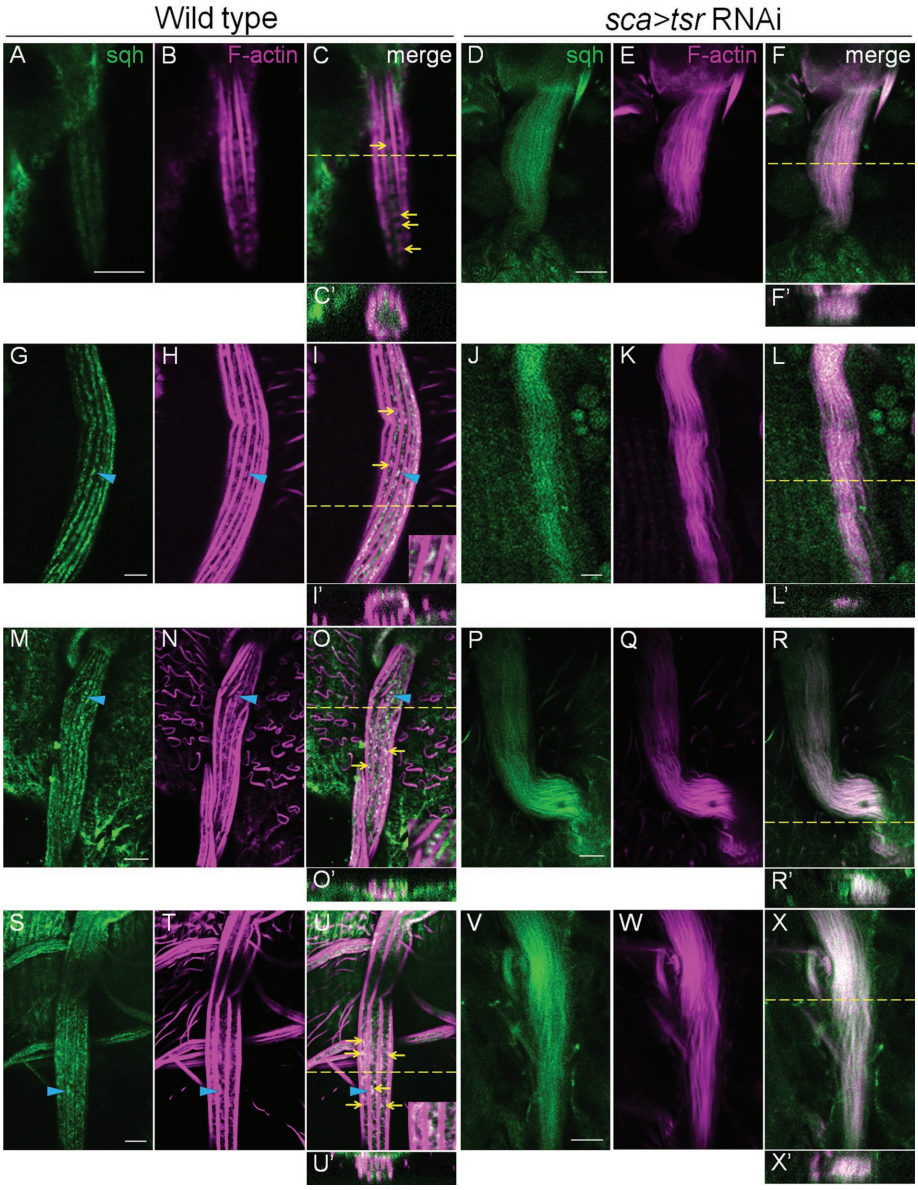

FIGURE 7: Cofilin deficiency resulted in myosin II–associated F-actin being incorporated into ectopic actin bundles. (A–X) Bristles of WT pupae expressing *sqh-GFP* (green) at 34 (A–C), 39 (G–I), 43 (M–O), and 48 (S–U) h APF stained with rhodamine-phalloidin (magenta) to reveal myosin II–associated actin snarls (yellow arrows). Blue arrowhead marks the place between bundles where a magnified view of myosin II colocalizing with actin snarls is shown in the inset at the bottom right. In contrast, cofilin deficiency resulted in strong colocalization of myosin II with the disorganized actin bundles in bristles at 34 (D–F), 39 (J–L), 43 (P–R), and 48 (V–X) h APF. Colocalization resulted in the merged color of white. Bars, 5 μm.

severed short actin filaments produced by cofilin could conceivably serve as actin nuclei and bypass the step of actin nucleation (a rate-limiting step), leading to fast and efficient polymerization of these short filaments by yet-unknown actin-polymerizing factors and subsequent cross-linking of these filaments into bundles.

The interplay between the dendritic actin network and actin bundles in the bristles as revealed by our study suggested that such interaction could similarly occur in other cell types in which these two different forms of actin cytoskeleton coexist. Indeed, a previous study on the filopodia of melanoma cells revealed that the dendritic actin network could be reorganized to initiate filopodial bundle formation (Svitkina *et al.*, 2003). Moreover, a study done in filopodia of neuronal growth cones found that the myosin II–associated actin network could affect the turnover and length of filopodial actin bundles (Medeiros *et al.*, 2006). Of interest, our recent study on the sarcomere of postnatal cardiomyocytes indicated that murine AIP1 was required for efficient actin filament addition to the thin filaments during postnatal myofibril growth (Yuan *et al.*, 2014). AIP1 deficiency resulted in excessively polymerized actin filaments within the sarcomeres, raising the possibility of an unidentified population of dynamic actin filaments (whose dynamics are regulated by cofilin and AIP1) interfering with the assembly of the stably capped and cross-linked linear actin filaments into the thin filaments.

MATERIALS AND METHODS

Drosophila genetics

Flies used in these studies were mostly raised on standard cornmeal agar medium and maintained under a 24-h cycle (light:dark, 12:12 h) at 25°C. All of the fly stocks were obtained from the Bloomington *Drosophila* Stock Center, except for the following: *flr RNAi*, *tsr RNAi*, *E-cad/shg RNAi* (Vienna *Drosophila* Resource Center; Tsinghua University RNAi Stock Center), flr^{BG}, $flr^{EY\text{-}P2}$, *GFP FRT80B/TM6B*, *AIP1-GFP* (Chu *et al.*, 2012), tsr^{null}, tsr^{ntf}, *GFP FRT42D* (Zhang *et al.*, 2011), *DE-Cadherin::GFP* (Huang *et al.*, 2009), *ubi-shg-GFP* (Kyoto *Drosophila* Genetic Resource Consortium), *sqh-GFP*, and *sqh-mCherry* (Martin *et al.*, 2009).

To generate *tsr* or *flr* mosaic clones, we used the FRT/Flp system and heat shock treatment. For example, *hs-Flp/Y*; *GFP FRT42D* males were crossed to *hs-Flp*; tsr^{null} *FRT42D/TSTL* females, which resulted in *hs-Flp/hs-Flp*; *GFP FRT42D*/tsr^{null} *FRT42D* progeny. Beginning at 3 d after egg laying, we heat shocked the larvae at 37°C for 2 h/d for 3 d. The hs-Flp induced mitotic recombination between FRT42D sites, which produced clones homozygous for tsr^{null} (GFP negative).

Light and scanning electron microscopies

Light microscopy pictures of adult flies were taken by an Olympus (Tokyo, Japan) BX51 microscope with a Motic MLC-150C Fiber Optic Cold Light Source (Xiamen, China). SEM pictures of adult bristles were taken by an S-3000N (Hitachi, Tokyo, Japan) in the SEM facility of Nanjing Agricultural University.

Dissection and immunohistochemistry

The preparation and dissection of pupal bristles were performed as described previously (Tilney *et al.*, 1996). The cut and cleaned thorax with bristles were fixed in 4% formaldehyde for 30 min, blocked with 10% normal goat serum in PBT (0.3% Triton X-100 in

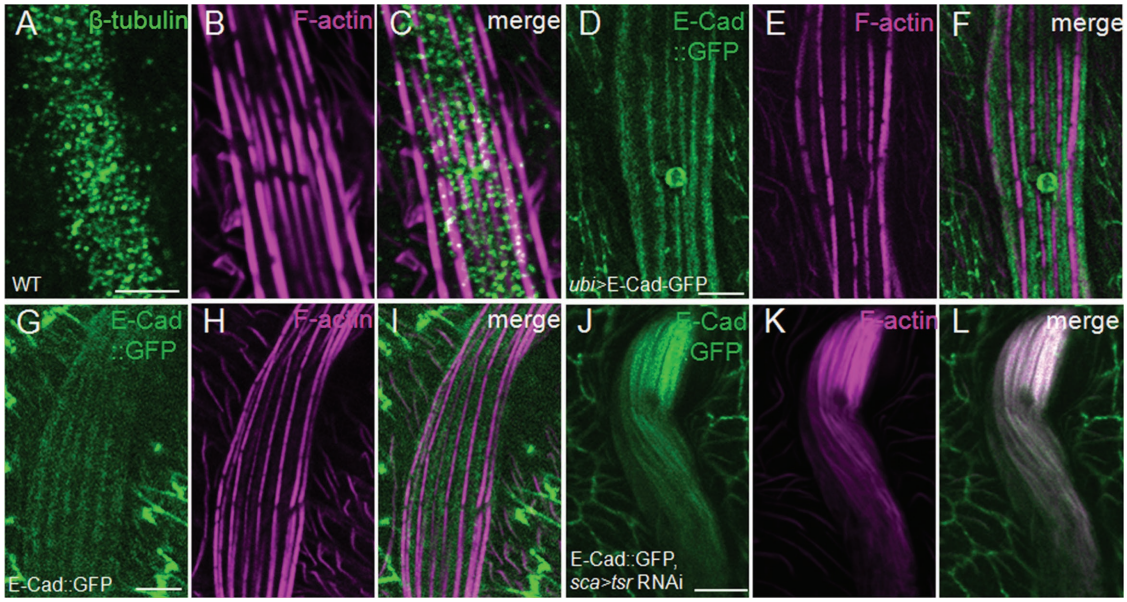

FIGURE 8: E-cad was distributed in a complementary manner to actin bundles at the membrane. (A–I) The cytoskeletal protein β-tubulin (A–C) had a diffuse and uniform distribution pattern, whereas exogenously expressed E-cad-GFP (D–F) and endogenously expressed E-cad-GFP (G–I) both had a distribution pattern complementary to the localization pattern of actin bundles. (J–L) Endogenously expressed E-cad–GFP relocated and colocalized with ectopic and disorganized actin bundles as a result of cofilin deficiency. All of the bristles shown are from 48–h APF pupae with the respective genotypes and were stained with phalloidin (magenta) and anti–β-tubulin antibody (A–C, green). Bars, 5 μm.

phosphate-buffered saline [PBS]) for 30 min and then incubated overnight at 4°C with the primary antibodies rabbit anti–total-cofilin antibody (1:100; Signalway Antibody, College Park, MD) and mouse anti–β-tubulin antibody (E7, 1:100; Developmental Studies Hybridoma Bank, Iowa City, IA). Cy3- or Cy5-conjugated secondary antibodies (1:200; Jackson ImmunoResearch Lab, West Grove, PA) were used to incubate tissues for 2 h at room temperature. F-actin was labeled by rhodamine-phalloidin (1:500; Sigma-Aldrich, St. Louis, MO) or fluorescein isothiocyanate–phalloidin (1:200; Sigma-Aldrich) for 1 h, and G-actin was labeled by DNaseI (1:200, Invitrogen, Carlsbad, CA) for 30 min. Then the tissues were washed with PBS and then mounted in 60% glycerol. Most of the confocal images were taken with a Leica (Wetzlar, Germany) SP5 II confocal microscope equipped with a HyD (sensitive to weak signals) detector, except for images in Figure 3, which were captured by an Olympus FV1000. *Z*-section images and cross-section reconstructions were analyzed with Leica Confocal Software.

Quantification of fluorescence signals

The fluorescence intensity (FI) of F-actin or G-actin staining is defined as the integrated signal density in each selected area divided by the selected area. The FI of F-actin or G-actin staining in each bristle was first measured for the respective genotypes (using ImageJ). An area in the adjacent notum epidermal epithelia, in which F-actin or G-actin staining is mostly uniform and predictable and does not vary greatly among different genotypes, was also chosen and measured for its FI. Then the normalized bristle FI was calculated as Bristle FI/ Epidermal FI. Finally, the average FIs of *tsr*- and *flr*-deficient bristles were further normalized against the average FI of WT bristles, with the average WT FI being 1.0.

ACKNOWLEDGMENTS

We are grateful to the Bloomington *Drosophila* Stock Center, the Vienna *Drosophila* Resource Center, the Tsinghua University RNAi Stock Center, Juan Huang, Yang Hong, and Adam Martin for fly stocks. This work was supported by Grants 31171335, 31271488, and 31571435 from the National Natural Sciences Foundation of China to J.C.

REFERENCES

Bamburg JR (1999). Proteins of the ADF/cofilin family: essential regulators of actin dynamics. Annu Rev Cell Dev Biol 15, 185–230.

Bartles JR, Zheng L, Li A, Wierda A, Chen B (1998). Small espin: a third actin-bundling protein and potential forked protein ortholog in brush border microvilli. J Cell Biol 143, 107–119.

Bretscher A, Weber K (1979). Villin: the major microfilament associated protein of the intestinal microvillus. Proc Natl Acad Sci USA 76, 2321–2325.

Bretscher A, Weber K (1980). Fimbrin, a new microfilament associated protein present in microvilli and other cell surface structures. J Cell Biol 86, 335–340.

Cant K, Knowles BA, Mooseker MS, Cooley L (1994). Drosophila singed, a fascin homolog, is required for actin bundle formation during oogenesis and bristle extension. J Cell Biol 125, 369–380.

Carlier MF, Laurent V, Santolini J, Melki R, Didry D, Xia G, Hong Y, Chua NH, Pantaloni D (1997). Actin depolymerizing factor (ADF/cofilin) enhances the rate of filament turnover: implication in actin-based motility. J Cell Biol 136, 1307–1322.

Chen J, Godt D, Gunsalus K, Kiss I, Goldberg M, Laski FA (2001). Cofilin/ADF is required for cell motility during Drosophila ovary development and oogenesis. Nat Cell Biol. 3, 204–209.

Chu D, Pan H, Wan P, Wu J, Luo J, Zhu H, Chen J (2012). AIP1 acts with cofilin to control actin dynamics during epithelial morphogenesis. Development 139, 3561–3571.

Frank DJ, Hopmann R, Lenartowska M, Miller KG (2006). Capping protein and the Arp2/3 complex regulate nonbundled actin filament assembly to indirectly control actin bundle positioning during *Drosophila melanogaster* bristle development. Mol Biol Cell 17, 3930–3939.

Guild GM, Connelly PS, Vranich KA, Shaw MK, Tilney LG (2002). Actin filament turnover removes bundles from Drosophila bristle cells. J Cell Sci 115, 641–653.
Huang J, Zhou W, Dong W, Watson AM, Hong Y (2009). Directed, efficient, and versatile modifications of the *Drosophila* genome by genomic engineering. Proc Natl Acad Sci USA 106, 8284–8289.
Hudson AM, Cooley L (2002). A subset of dynamic actin rearrangements in *Drosophila* requires the Arp2/3 complex. J Cell Biol 156, 677–687.
Maciver SK, Zot HG, Pollard TD (1991). Characterization of actin filament severing by actophorin from Acanthamoeba castellanii. J Cell Biol 115, 1611–1620.
Martin AC, Kaschube M, Wieschaus EF (2009). Pulsed contractions of an actin-myosin network drive apical constriction. Nature 457, 495–499.
Medeiros NA, Burnette DT, Forscher P (2006). Myosin II functions in actin-bundle turnover in neuronal growth cones. Nat Cell Biol 8, 215–226.
Okada K, Obinata T, Abe H (1999). XAIP1: a Xenopus homologue of yeast actin interacting protein 1 (AIP1), which induces disassembly of actin filaments cooperatively with ADF/cofilin family proteins. J Cell Sci 112, 1553–1565.
Ono S (2003). Regulation of actin filament dynamics by actin depolymerizing factor/cofilin and actin-interacting protein 1: new blades for twisted filaments. Biochemistry 42, 13363–13370.
Revenu C, Athman R, Robine S, Louvard D (2004). The co-workers of actin filaments: from cell structures to signals. Nat Rev Mol Cell Biol 5, 1–12.
Rodal AA, Tetreault JW, Lappalainen P, Drubin DG, Amberg DC (1999). Aip1p interacts with cofilin to disassemble actin filaments. J Cell Biol 145, 1251–1264.
Svitkina TM, Bulanova EA, Chaga OY, Vignjevic DM, Kojima S, Vasiliev JM, Borisy GG (2003). Mechanism of filopodia initiation by reorganization of a dendritic network. J Cell Biol 160, 409–421.
Theodosiou NA, Xu T (1998). Use of FLP/FRT system to study *Drosophila* development. Methods 14, 355–365.
Tilney LG, Connelly PS, Ruggiero L, Vranich KA, Guild GM, Derosier D (2004). The role actin filaments play in providing the characteristic curved form of Drosophila bristles. Mol Biol Cell 15, 5481–5491.
Tilney LG, Connelly PS, Ruggiero L, Vranich KA, Guild GM (2003). Actin filament turnover regulated by cross-linking accounts for the size, shape, location, and number of actin bundles in Drosophila bristles. Mol Biol Cell 14, 3953–3966.
Tilney LG, Connelly P, Smith S, Guild GM (1996). F-actin bundles in *Drosophila* bristles are assembled from modules composed of short filaments. J Cell Biol 135, 1291–1308.
Tilney LG, Connelly PS, Vranich KA, Shaw MK, Guild GM (2000). Regulation of actin filament cross-linking and bundle shape in *Drosophila* bristles. J Cell Biol 148, 87–100.
Tilney LG, DeRosier DJ (2005). How to make a curved *Drosophila* bristle using straight actin bundles. Proc Natl Acad Sci USA 102, 18785–18792.
Tilney LG, Tilney MS, Guild GM (1995). F actin bundles in Drosophila bristles. I. Two filament cross-links are involved in bundling. J Cell Biol 130, 629–638.
Wang W, Eddy R, Condeelis J (2007). The cofilin pathway in breast cancer invasion and metastasis. Nat Rev Cancer 7, 429–440.
Xu J, Wan P, Wang M, Zhang J, Gao X, Hu B, Han J, Chen L, Sun K, Wu J, *et al*. (2015). AIP1-mediated actin disassembly is required for postnatal germ cell migration and spermatogonial stem cell niche establishment. Cell Death Dis 16, e1818.
Yuan B, Wan P, Chu D, Nie J, Cao Y, Luo W, Lu S, Chen J, Yang Z (2014). A cardiomyocyte-specific *Wdr1* knockout demonstrates essential functional roles for actin disassembly during myocardial growth and maintenance in mice. Am J Pathol 184, 1967–1980.
Zhang L, Luo J, Wan P, Wu J, Laski F, Chen J (2011). Regulation of cofilin phosphorylation and asymmetry in collective cell migration during morphogenesis. Development 138, 455–464.
Zheng L, Sekerková G, Vranich K, Tilney LG, Mugnaini E, Bartles JR (2000). The deaf jerker mouse has a mutation in the gene encoding the espin actin-bundling proteins of hair cell stereocilia and lacks espins. Cell 102, 377–385.